J|A|C|S
ARTICLES

Published on Web 12/31/2009

Ligand-Controlled Polytypism of Thick-Shell CdSe/CdS Nanocrystals

Benoît Mahler,[†] Nicolas Lequeux,[‡] and Benoît Dubertret*,[†]

Laboratoire de Physique et d'Etude des Matériaux, CNRS UPR5, ESPCI 10 rue Vauquelin, 75231 Paris, France, and Laboratoire Physicochimie des Polymères et Milieux Dispersés, UMR 7615, ESPCI 10 rue Vauquelin, 75231 Paris, France

Received April 30, 2009; E-mail: Benoit.dubertret@espci.fr

Abstract: We report the synthesis of CdSe/CdS semiconductor core/shell nanocrystals with very thick (5 nm) CdS shells. As in the case of core CdSe nanocrystals, we show that a thick-shell CdSe/CdS core/shell structure can be synthesized in either a pure wurtzite (W) or a zinc-blende (ZB) crystal structure. While the growth of thick-shell wurtzite CdSe/CdS is quite straightforward, we observe that the growth of a CdS shell on zinc-blende CdSe cores is more difficult and leads to wurtzite/zinc-blende polytypism when primary amines are present during the shell formation. Using absorption spectra analysis to differentiate zinc blende from wurtzite CdSe, we show that primary amines can induce a nearly complete structural transformation of CdSe ZB cores into W cores. This better understanding of the CdSe ligand-dependent crystal structural evolution during shell growth is further used to grow large (10 nm)-diameter perfect zinc-blende CdSe core crystals emitting above 700 nm, and perfect ZB thick-shell CdSe/CdS nanocrystals. We observed that all thick-shell CdSe/CdS QDs have extremely reduced blinking events compared to thin-shell QDs, without any significant influence of crystalline structure and polytypism.

Introduction

The synthesis of semiconductor nanoparticles (quantum dots or QDs) with controlled size, shape, and crystallinity is well documented,[1] although a detailed understanding of the growth process is not yet available. QDs physicochemical properties can be further tuned and optimized by growing a semiconductor shell on the QD core to obtain a core/shell structure.[2] While most of the work on QD synthesis has been focused on QD core systems, less has been done on core/shell nanoparticles. Core/shell structures are important, however; they usually have better resistance to photobleaching and higher quantum yield, and the QD fluorescence has better resistance to surface modifications.[3] Moreover, it has been shown recently, that CdSe/CdS QDs with thick (5 nm), carefully grown shells have extremely reduced blinking when observed at the single nanoparticle level.[4,5] These observations motivate the development of methods to synthesize QDs with thick (>5 nm) epitaxially grown shells with a controlled crystal structure.

Three parameters have to be considered when growing core/shell materials: (i) the lattice mismatch between the crystal core and the crystal that makes the shell, (ii) the band alignment between the core material and the shell material, and finally (iii) the crystal structure evolution during shell growth. Each of these parameters has to be optimized to obtain core/shell QDs with controlled size, shape, and physical properties. The influence of the first two parameters has already been studied in detail. For example, the lattice mismatch between the core and the shell induces radial pressure in the QD that can be as high as 4 GPa when the lattice mismatch between the core and the shell is just 7%.[6] Low lattice mismatch or gradual lattice mismatch adaptation via multishell[7] or gradient shells[8] is thus important if thick crystalline shells are to be grown. Different band alignments between the core and the shell give access to wave function engineering and type II semiconductor nanocrystals where the electron and the hole are spatially separated.[9] To the best of our knowledge, no studies have yet tackled the problem of crystal structure evolution when a thick shell is grown on a core.

Experimental Section

Chemicals. 1-Octadecene (ODE, 90%, Aldrich), trioctylamine (TOA, 98%, Fluka), oleylamine (70%, Fluka), oleic acid (90%, Aldrich), trioctylphosphine (TOP, 90%, Cytec), trioctylphosphine oxide (TOPO, 90%, Cytec), sodium myristate (99%, Fluka), cadmium nitrate (99.999%, Aldrich), cadmium oxide (99.99%,

[†] Laboratoire de Physique et d'Etude des Matériaux, CNRS UPR5.
[‡] Laboratoire Physicochimie des Polymères et Milieux Dispersés, UMR 7615.

(1) Yin, Y.; Alivisatos, A. P. *Nature* **2005**, *437*, 664–670.
(2) Hines, M. A.; Guyot-Sionnest, P. *J. Phys. Chem.* **1996**, *100*, 468–471.
(3) Dabbousi, B. O.; Rodriguez-Viejo, J.; Mikulec, F. V.; Heine, J. R.; Mattoussi, H.; Ober, R.; Jensen, K. F.; Bawendi, M. G. *J. Phys. Chem. B* **1997**, *101*, 9463–9475.
(4) Mahler, B.; Spinicelli, P.; Buil, S.; Quelin, X.; Hermier, J.-P.; Dubertret, B. *Nat. Mater.* **2008**, *7*, 659–664.
(5) Chen, Y.; Vela, J.; Htoon, H.; Casson, J. L.; Werder, D. J.; Bussian, D. A.; Klimov, V. I.; Hollingsworth, J. A. *J. Am. Chem. Soc.* **2008**, *130*, 5026–5027.
(6) Ithurria, S.; Guyot-Sionnest, P.; Mahler, B.; Dubertret, B. *Phys. Rev. Lett.* **2007**, 99.
(7) Han, L.; Qin, D.; Jiang, X.; Liu, Y.; Wang, L.; Chen, J.; Cao, Y. *Nanotechnology* **2006**, 4736.
(8) Xie, R. G.; Kolb, U.; Li, J. X.; Basche, T.; Mews, A. *J. Am. Chem. Soc.* **2005**, *127*, 7480–7488.
(9) Kim, S.; Fisher, B.; Eisler, H. J.; Bawendi, M. *J. Am. Chem. Soc.* **2003**, *125*, 11466–11467.

Aldrich), selenium pellets (99.99%, Aldrich), sulfur (99.998% Aldrich), and tetradecylphosphonic acid (TDPA, 97%, PCI synthesis) were used as received.

Precursors Preparation. Cadmium myristate was prepared according to a previously published procedure.[10] A solution of cadmium oleate in oleic acid was synthesized by heating 1.45 g CdO in 20 mL oleic acid at 170 °C under argon for 1 h until it turned colorless. The solution was then degassed under vacuum at 100 °C. TOPSe 1 M in TOP was prepared by dissolving 7.9 g Se powder in 100 mL TOP under magnetic stirring. Similarly, TOPS 0.5 M in TOP was obtained by dissolving 1.6 g sulfur in 100 mL TOP. Sulfur stock solution in ODE (0.1 M) was prepared by heating 320 mg of sulfur in 100 mL degassed ODE at 120 °C until complete dissolution.

Protocol 1, Synthesis of Wurtzite Structure Nanocrystals. Nanocrystals were synthesized by a rapid injection of a mixture of 4 mL TOPSe 1 M in TOP, 3 mL oleylamine, and 1 mL octadecene into a degassed solution of 750 μL $Cd(oleate)_2$ 0.5 M in oleic acid, 8 mL octadecene, and 1.2 mL TOPO at 300 °C. The growing CdSe nanocrystals were then maintained at 270 °C until the desired size was obtained (typically 3-nm diameter). After precipitation with ethanol, the dots were suspended in 10 mL hexane.

Protocol 2, Synthesis of CdSe Zinc-Blende Structure Nanocrystals. NCs were prepared by a procedure adapted from Cao et al.[10] Typically, a mixture of 16 mL ODE, 0.3 mmol of cadmium myristate, and 0.15 mmol Se powder, 100 mesh, was degassed on vacuum at room temperature during 1 h and heated under argon flow up to 240 °C during 10 min. One milliliter of oleic acid was added dropwise during the growth. After reaction the mixture was allowed to cool to room temperature, and NCs were precipitated using ethanol. The precipitate was dispersed in 10 mL hexane. Small variations of this protocol gave access to CdSe QDs with sizes ranging from 1.5 to 10 nm (See Supporting Information).

Synthesis of Thick-Shell CdSe/CdS Using Successive Ion Layer Adsorption and Reaction (SILAR)[11] Protocol. Typically, 2 mL hexane solution of bare CdSe nanocrystals (100 μM), 4 mL octadecene, and 2 mL oleylamine was degassed at 70 °C during one hour. The solution was then heated to 230 °C under argon atmosphere. Successive injections of $Cd(oleate)_2$ stock solution and sulfur stock solution (0.1 M in ODE) allowed the shell to grow monolayer by monolayer. The reaction time was adjusted to allow complete reaction of the precursors injected (typically 10 min between two injections).

Synthesis of Thick-Shell CdSe/CdS Using Continuous Injection. Two milliliters of hexane solution of CdSe nanocrystals (35 μM), 8 mL trioctylamine, and 600 μL $Cd(oleate)_2$ 0.5 M in oleic acid were degassed at 70 °C during one hour. The solution was then heated to 260 °C (or 280 °C to obtain spherical nanocrystals) under argon atmosphere, and a mixture of 3.4 mL TOA, 600 μL TOPS 0.5 M in TOP, and 1 mL oleic acid was injected in 4 h.

Ligand-Induced CdSe Crystal Structure Transition from Zinc-Blende to Wurtzite. A mixture containing 3 mL ODE, 2 mL oleylamine, and 1 mL zinc-blende (ZB) CdSe nanocrystals (about 100 μM) was degassed 30 min at 70 °C. Under argon, the solution was then heated by 20-min steps at: 100, 120, 150, 170, and 200 °C. Samples were taken before and after each temperature step.

Characterizations. Absorption measurements were realized on a Cary 5E UV−visible spectrometer, and fluorescence and photoluminescence excitation (PLE) spectra were measured with a Jobin-Yvon Horiba fluoromax 3. All transmission electron microscopy (TEM) were taken using a TEM JEOL 2010 with field electron gun. Powder X-ray diffraction (PXRD) experiments are realized with a Philips X'Pert diffractometer with Cu Kα source.

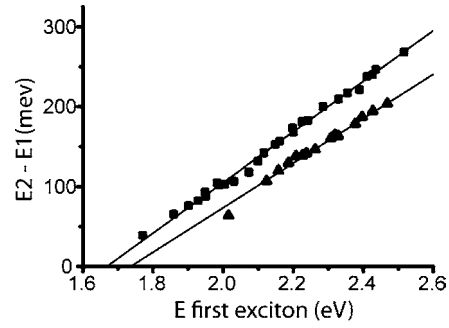

Figure 1. Energy difference between the first and the second exciton obtained after a fit of the low-energy part of the absorption spectra with three Gaussians versus the energy (E_1) of the first exciton for wurtzite (triangles) and zinc-blende (squares) CdSe nanocrystals. For each crystal structures, QDs with diameters ranging from 1.5 to 8 nm have been analyzed. The two lines are the linear fits for each data set (see Supporting Information for the detailed fitting procedure).

Results and Discussion

Spectroscopic Determination of Wurtzite and Zinc-Blende CdSe Crystal Structure. CdSe semiconductors exist in two different crystalline structures at ambient temperature:[12] wurtzite (W, hexagonal symmetry) and zinc-blende (ZB, cubic symmetry). They often present a polytypism between the two phases due to low internal energy differences (<20 meV per atom) and small structural variations (position of the fourth neighbor). The crystal structure of large QDs can easily be obtained using PXRD measurements or high-resolution transmission electron microscopy (HRTEM) observations. Unfortunately, the use of these techniques is much more complicated on smaller dots due to higher signal-to-noise ratios and broadening of X-ray diffraction patterns. Interestingly, the small structural variations between the W and the ZB structures lead to significant electronic and optic differences,[13] and changes in symmetry groups modify the degeneracy of bands especially for ground hole states.[14] As a consequence, for a given particle size, the energy difference ΔE_{2-1} between the first and the second excitons is different for ZB and W structures in II−VI semiconductors.[15−17] Such difference is confirmed in Figure 1. To a first approximation, ΔE_{2-1} varies linearly as a function of the first exciton energy E_1, both for ZB and W structures. Furthermore the value of the fit at $\Delta E_{2-1} = 0$ is 1.74 eV for W, in excellent agreement with literature values for CdSe wurtzite band gap energy at room temperature. The linear extrapolation at $\Delta E_{2-1} = 0$ for CdSe ZB gives a value of 1.67 eV which is

(10) Yang, Y. A.; Wu, H. M.; Williams, K. R.; Cao, Y. C. *Angew. Chem., Int. Ed.* **2005**, *44*, 6712–6715.
(11) Li, J. J.; Wang, Y. A.; Guo, W. Z.; Keay, J. C.; Mishima, T. D.; Johnson, M. B.; Peng, X. G. *J. Am. Chem. Soc.* **2003**, *125*, 12567–12575.
(12) Yeh, C.-Y.; Lu, Z. W.; Froyen, S.; Zunger, A. *Phys. Rev. B J1 - PRB* **1992**, *46*, 10086 LP–10097.
(13) Ninomiya, S.; Adachi, S. *J. Appl. Phys.* **1995**, *78*, 4681–4689.
(14) Efros, A. L.; Rosen, M.; Kuno, M.; Nirmal, M.; Norris, D. J.; Bawendi, M. *Phys. Rev. B J1 - PRB* **1996**, *54*, 4843 LP–4856.
(15) Norris, D. J.; Bawendi, M. G. *Phys. Rev. B J1 - PRB* **1996**, *53*, 16338–16346.
(16) Jasieniak, J.; Bullen, C.; van Embden, J.; Mulvaney, P. *J. Phys. Chem. B* **2005**, *109*, 20665–20668.
(17) Mohamed, M. B.; Tonti, D.; Al-Salman, A.; Chemseddine, A.; Chergui, M. *J. Phys. Chem. B* **2005**, *109*, 10533–10537.

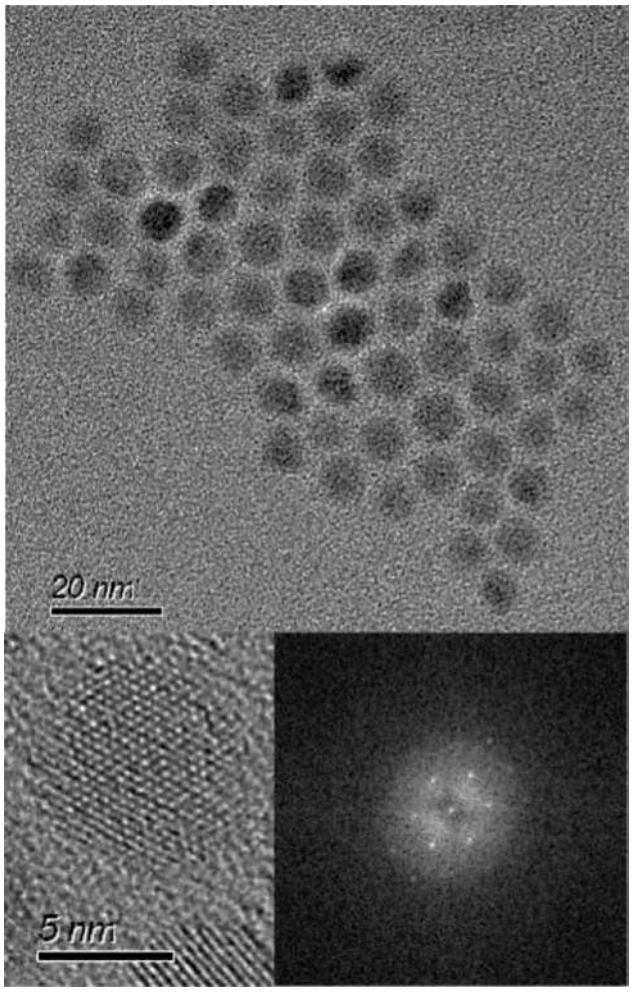

Figure 2. TEM and HRTEM images of W CdSe (3-nm diameter)/CdS (2.5-nm thick) nanocrystals. The fast Fourier transform (FFT) of HRTEM corresponds to [001] zone axis, characteristic of wurtzite structure.

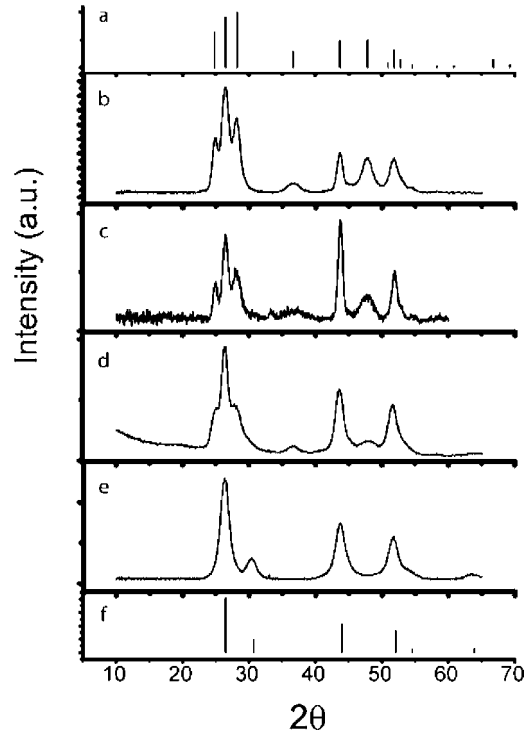

Figure 3. PXRD diffractograms for the different CdSe/CdS nanocrystals synthesized. (a, f) Bulk diffraction peaks for W and ZB CdS, respectively. (b) W CdSe/CdS sample (3-nm CdSe core and 2.5-nm CdS shell). (c, d) Polytypic CdSe/CdS samples obtained with different ZB core sizes; (c) is 2.5-nm CdSe core and 4-nm CdS shell, (d) is 4-nm CdSe core and 2.5-nm CdS shell). (e) Pure ZB CdSe/CdS sample (3-nm CdSe core and 2.5-nm CdS shell).

also in excellent agreement with most literature values for the band gap energy of CdSe ZB at 300 K (1.66 eV).[18−20] We can then use this spectroscopic measurement to accurately and easily determine the crystalline phase of a CdSe QDs sample as small as 2-nm diameter, which is impossible by conventional techniques such as HRTEM or PXRD.

Growth of a Thick-Shell CdS on a Wurtzite CdSe Core. The synthesis of thin core/shell semiconductor nanocrystals with a W crystal structure is well documented.[3,11] However, to the best of our knowledge, no synthesis of thick shell (>4 nm) has been reported so far with control of the core/shell crystal structure. The core synthesis described here (protocol 1) is a modification of a Li protocol,[11] which is known to produce W CdSe cores. The growth of an epitaxial CdS shell is achieved by a SILAR process that produces spherical, monodisperse, and wurtzite CdSe/CdS nanocrystals (Figure 2). The HRTEM image reveals the synthesis of defect-free nanocrystals (Figure 2), and the excellent crystallinity of the CdSe/CdS is confirmed by powder XRD measurement (Figure 3b). Remarkably, relative intensities of the peaks ($2\bar{1}0$) and (103) indicate that this shell synthesis perfectly conserves the wurtzite structure and does not generate any stacking faults perpendicularly to the [001] direction which would have decreased the intensity of the (103) peak.[21] We thus confirm that, on wurtzite CdSe nanocrystals, a SILAR protocol permits the growth of a thick, perfectly crystalline, W CdS shell.

Apparition of Polytypism during Growth of CdS Shell on Zinc-Blende CdSe Cores. Much less has been done on the shell growth on CdSe ZB cores. Indeed, the first "user friendly" protocols describing the synthesis of zinc-blende CdSe nanocrystals dates back to 2005.[10,16,17,22] While we expected that the same procedure used to grow a W CdS shell on W CdSe could be used to grow a ZB shell on ZB CdSe, we found that it was not the case. On small (<3-nm diameter) ZB CdSe nanocrystals obtained with protocol 2, the use of a SILAR protocol induces the formation of highly polytypic nanocrystals as revealed by the PXRD measurements (Figure 3c). We can see the coexistence of characteristic peaks of both ZB and W structures. Interestingly, common peaks are sharper than pure wurtzite ones; these diffraction planes are not perturbed by the presence of stacking faults along the ZB [111] axis. The TEM image (Figure 4) confirms that the presence of both structures is not due to a mixture of purely wurtzite and zinc-blende nanocrystals; the sample is highly homogeneous, and there is

(18) Shan, W.; Song, J. J.; Luo, H.; Furdyna, J. K. *Phys. Rev. B J1 - PRB* **1994**, *50*, 8012 LP–8015.
(19) Kim, Y. D.; Klein, M. V.; Ren, S. F.; Chang, Y. C.; Luo, H.; Samarth, N.; Furdyna, J. K. *Phys. Rev. B J1 - PRB* **1994**, *49*, 7262 LP–7270.
(20) Lunz, U.; Kuhn, J.; Goschenhofer, F.; Schussler, U.; Einfeldt, S.; Becker, C. R.; Landwehr, G. *J. Appl. Phys.* **1996**, *80*, 6861–6863.
(21) Murray, C. B.; Norris, D. J.; Bawendi, M. G. *J. Am. Chem. Soc.* **1993**, *115*, 8706–8715.
(22) Deng, Z.; Cao, L.; Tang, F.; Zou, B. *J. Phys. Chem. B* **2005**, *109*, 16671–16675.

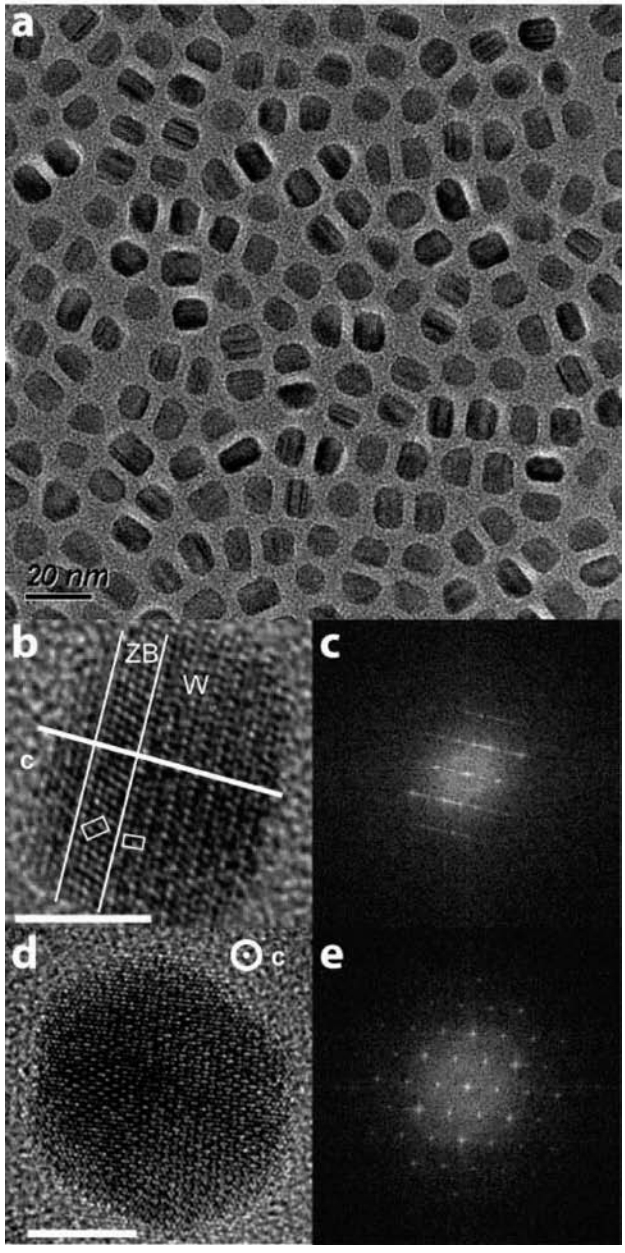

Figure 4. (a) Polytypic CdSe (3-nm diameter)/CdS (4-nm thick) nanocrystals.The TEM image reveals a hexagonal prismatic shape. (b) HRTEM image highlights the presence of wurtzite [$2\bar{1}0$] and zinc-blende [$01\bar{1}$] domains when the observation is done perpendicularly to the W *c*-axis. Unit cells are drawn in white. (c) Polytypism appears in FFT as blurred lines. (d) Along the W *c*-axis it is impossible to distinguish W or ZB, the overall structure appears wurtzite in the FFT (e). Scale bar on HRTEM pictures is 5 nm.

no secondary nucleation. HRTEM images (Figure 4) demonstrate the coexistence of wurtzite and zinc-blende domains within single nanocrystals.

Silar protocol on larger (>4 nm) ZB CdSe dots also leads to a pronounced polytypism. The powder diffractogram of this sample (Figure 3d) shows well-resolved zinc-blende structure peaks but broader wurtzite ones. The nanocrystals synthesized are monodisperse and rod-shaped (Figure 5) with a small aspect ratio (about 1.5). Stacking faults are clearly visible, and it is possible to distinguish W and ZB domains. Surprisingly, the geometry of the nanocrystals (rodlike) corresponds to the wurtzite structure, where the *c*-axis is the growth direction.

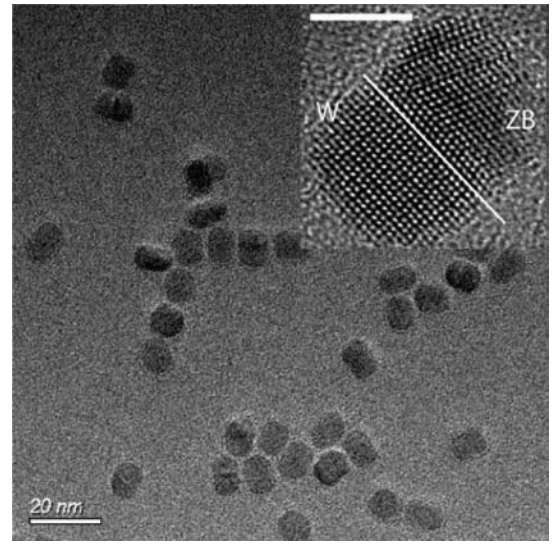

Figure 5. TEM image of polytypic CdSe (4-nm diameter)/CdS synthesized using larger ZB CdSe cores. The nanocrystals are rod shaped, and we can distinguish the coexistence of a wurtzite and a zinc-blende domain on the HRTEM image (inset) Scale bar on the HRTEM picture is 5 nm.

We concluded that SILAR protocol for the growth of a CdS shell on ZB CdSe cores induces partial crystalline transition from zinc-blende to wurtzite which disturbs the epitaxial growth and leads to polytypic non-isotropic nanostructures. To obtain thick-shell, perfect ZB CdSe/CdS nanocrystals we have to change the type of shell synthesis.

Ligand-Driven Crystalline Transition. A main difference between the wurtzite and zinc-blende protocols described above is the presence of oleylamine to obtain wurtzite CdSe and CdSe/CdS nanocrystals. We therefore hypothesized that the presence of primary amines during the shell growth on ZB CdSe cores was responsible for the polytypism observed on Figures 4 and 5. If this hypothesis is correct, two scenarios are possible: (i) the primary amines induce a partial core crystal structure change from ZB to W, and then the shell grows in a mixture of ZB and W structure, or (ii) the ZB core remains unaffected by the primary amines but the shell tends to grow with a W structure because of the presence of primary amines. To find out which scenario was correct, we performed the following experiment: a 2.2 nm diameter CdSe ZB core sample synthesized with protocol 2 was introduced at room temperature under argon in an ODE/oleylamine mixture, and slowly heated by steps to 200 °C as described in the Experimental Section. At each temperature step, an absorption spectrum was recorded, and the evolution of $E_2 - E_1$ vs E_1 was monitored (Figure 6b). The first exciton position is found to strongly red-shift as the temperature increases, a trend that we interpret as Ostwald ripening, while the energy difference $E_2 - E_1$ decreases so that at 200 °C, the QDs appear to be almost perfectly W.

It is hard to conclude if we assisted in a global crystalline reorganization or if the Ostwald ripening-induced growth leads to a mixed structure with a zinc-blende core and a wurtzite shell. The same experiment performed with a 3-nm diameter sample (Figure 6c) exhibits a slightly different behavior. We do not assist in an Ostwald ripening, but a partial dissolution of the dots occurs with a decrease of ΔE_{2-1}, indicating a partial crystalline transition. Finally, for a sample containing large (6-nm diameter) QDs (Figure 6d), heating in the presence of amines

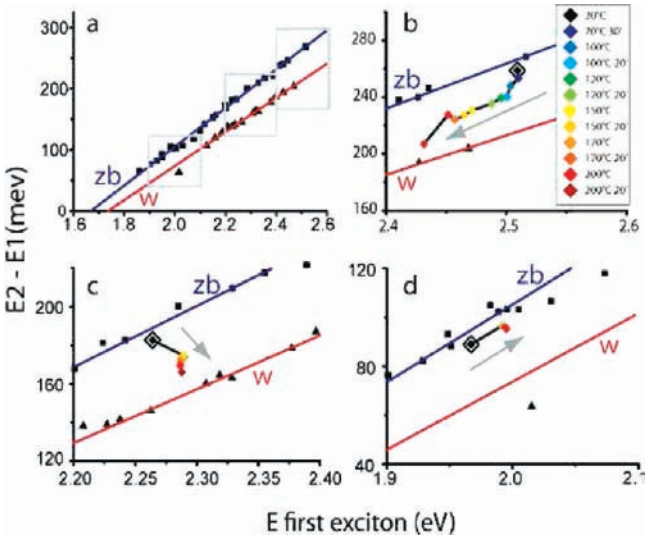

Figure 6. (a) Same as Figure 1 (b−d): annealing effect on ΔE_{2-1} for 2.2-, 3-, and 6-nm diameter ZB CdSe nanocrystals. The starting point (room temperature) of each experiment is indicated using a double square.

only leads to partial QD dissolution without any measurable crystalline change.

Differences of behavior observed between the samples of different sizes during ligand exchange and annealing suggest that the crystalline transition observed is surface driven. The higher the surface-to-volume ratio, the more effective the crystalline transition. This crystalline transition takes place even though the ligand exchange is not total: even after heating at 180 °C, some carboxylic acids remain on the QD surface as we can see in FT-IR measurement (see Supporting Information, Figure S3). This ligand exchange can occur during the degassing and heating steps of shell growth procedures using amines and induces a partial crystalline transition before the effective growth of the shell. We therefore think that scenario 1 is happening. We conclude that to preserve the core crystal structure, shell growth on CdSe ZB QDs must be done in the absence of primary amines. This is a necessary condition.

Perfect Zinc-Blende CdSe/CdS Core/Shell Nanocrystals. To test whether the absence of primary amines is a sufficient condition for preserving the core crystal structure using the shell growth, we have shown that a slow injection of TOPS 0.5 M in a solution of ZB CdSe cores (3-nm diameter) in trioctylamine and $(Cd(oleate)_2$ at 260 °C under argon flux induces the growth of CdS shell with perfectly ZB core/shell structure. At this reaction temperature the nanocrystals are monodisperse and tetrahedral in shape (Figure 7). They exhibit a high crystallinity as shown in the HRTEM images, and the structure is indeed zinc-blende as determined by powder XRD (Figure 3e) and FFT of the HRTEM image (inset, Figure 6). The shape of the nanocrystals can then be partially controlled by the reaction temperature. Working at 300 °C allows us to synthesize spherical zinc-blende CdSe/CdS QDs (see Supporting Information).

Discussion

Since the first organometallic synthesis of colloidal semiconductor nanocrystals,[21] the influence of ligands during nucleation and growth has been extensively studied. A judicious choice of such molecules allows a fine control of nucleation rate, precursor reactivity, growth rate, and final geometry of

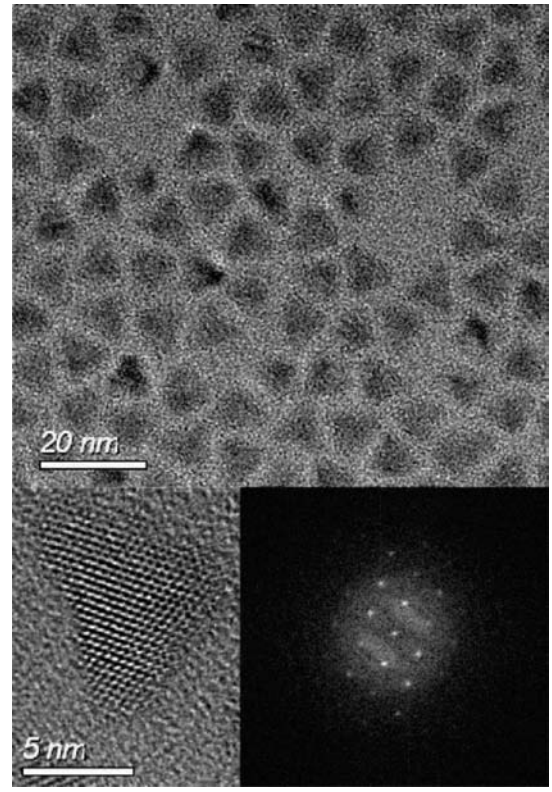

Figure 7. TEM picture of perfect ZB CdSe/CdS tetrahedral nanocrystals (edge length: 9 nm). FFT of HRTEM image reveals a characteristic [110] zone axis.

QDs. A wide collection of shapes ranging from rods[23] and tetrapods[24] to platelets[25] has been synthesized. The driving force of such syntheses is the modulation of relative reactivities of nanocrystal facets by the use of strongly bonded ligands which slow down the growth on some crystal directions.[24] Rods and tetrapods are then obtained by using phosphonic acids (generally hexylphosphonic acid) to poison the $w(100)$ planes. On the other hand, platelets can be obtained by a low-temperature reaction of a mixture containing cadmium acetate and fatty carboxylic acid with a Se precursor.

The results presented above highlight another effect of the ligands not described thus far. Here, the action of primary amines is first to promote a zinc-blende-to-wurtzite crystalline transition and second to induce a subsequent wurtzite shell growth. Depending on the CdSe nanocrystallite size, when we anneal ZB CdSe QDs in oleylamine, we can observe an almost total phase transition (CdSe of 2.2 nm diameter, surface-to-volume ratio $S/V = 0.62$), a partial phase transition (3-nm diameter, $S/V = 0.49$), or no transition for larger nanocrystals (6 nm, $S/V = 0.27$). The transition is then clearly surface driven. We can hypothesize that a modification of surface ligand nature and coverage induces a different surface relaxation and equilibrium state for the whole nanocrystal.[26] If the effect is strong enough, we can assist in a phase transition toward the

(23) Peng, X. G.; Manna, L.; Yang, W. D.; Wickham, J.; Scher, E.; Kadavanich, A.; Alivisatos, A. P. *Nature* **2000**, *404*, 59–61.
(24) Manna, L.; Milliron, D. J.; Meisel, A.; Scher, E. C.; Alivisatos, A. P. *Nat. Mater.* **2003**, *2*, 382–385.
(25) Ithurria, S.; Dubertret, B. *J. Am. Chem. Soc.* **2008**, *130*, 16504–16505.
(26) Puzder, A.; Williamson, A. J.; Zaitseva, N.; Galli, G.; Manna, L.; Alivisatos, A. P. *Nano Lett.* **2004**, *4*, 2361–2365.

thermodynamically stable wurtzite structure. Indeed, for bulk CdSe the transition temperature from ZB to W is 95 ± 5 °C,[27] and it has been shown that the transition temperature is about 200 °C for a 3-nm mean diameter nanocrystallite CdSe powder without ligands.[28] It is noteworthy that carboxylic acid-stabilized ZB CdSe QDs are at least stable up to 300 °C, and subsequent growth at this temperature allows the conservation of the ZB structure (see Supporting Information). The main parameter controlling the crystal structure of CdSe nanocrystals appears to be the nature of surface ligands[29] rather than the temperature. Particularly, fatty carboxylic acids seem to stabilize the ZB structure, while fatty primary amines favor the W structure.

The synthesis of CdS shell on core CdSe nanocrystals follows the same pathway. A partial crystalline transition can occur during the heating and the degassing steps, depending on the CdSe nanocrystal radius. Then the subsequent CdS growth leads to a majority of W nanocrystals with stacking faults (inducing the presence of small ZB domains) if the core is small enough to have undergone crystalline transition (nanocrystals Figure 4). On larger nanocrystals, the core remains zinc-blende, and we assist in a wurtzite CdS growth on one side of the core (CdSe/CdS Figure 5 and Figure S1, Supporting Information) due to energetically favorable growth in the W structure and the slow injection of precursors (SILAR) preventing the obtention of tetrapod shapes.[30,31] Using XPS analysis, we confirmed the homogeneous growth of a thick CdS shell on the CdSe core (see Supporting Information).

Growth of Large CdSe ZB QDs. Finally, we applied this better understanding of the shell growth to the synthesis of large (15-nm edge length) pyramidal-shaped ZB CdSe cores (See Supporting Information). Starting from ZB CdSe QDs synthesized with protocol 2, we slowly injected Se ODE and $Cd(oleate)_2$ in the core mixture to obtain perfectly ZB CdSe QDs emitting with a maximum at 707 nm, which is, as far as we know, the reddest emission obtained with CdSe nanocrystals. These results confirm that the ZB CdSe band gap is indeed smaller than the W CdSe one and that large ZB CdSe QDs can be easily grown using a one-step injection if no primary amines are used during the growth.

Optical Properties of Thick-Shell CdSe/CdS. Shell growth can be simply monitored by observing red-shift on fluorescence spectra and the increase of absorption cross section at energies higher than the CdS band gap (2.5 eV, 496 nm). These features are respectively due to electron delocalization into the whole core/shell nanocrystal and excitonic transfer from the shell to the core prior to radiative recombination. It is noteworthy that optical properties of the resulting CdSe/CdS core/shell nanocrystals are well conserved. Particularly, the quantum yields of the different samples are always quite high (50−70%) without any significant correlation between QY and polytypism. The apparition of stacking faults in the nanocrystal is not followed by creation of nonradiative recombination centers which would decrease the quantum efficiency.

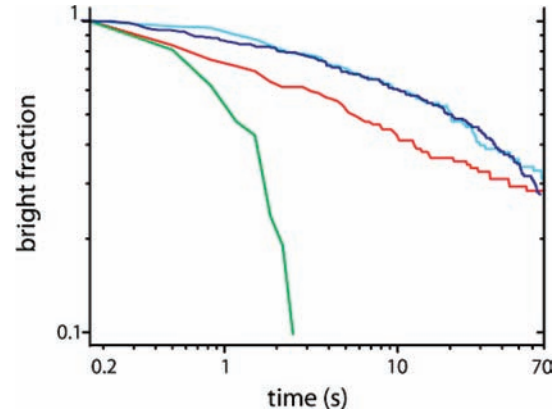

Figure 8. Percentage of QDs that have not blinked vs time for CdSe/ZnS nanocrystals (620 nm emission, 0.5 nm ZnS thickness) (green), zinc-blende CdSe/CdS NCs (sample imaged Figure 6 in red, about 3-nm thick CdS shell) polytypic CdSe/CdS NCs (sample imaged Figure 4 in blue and sample imaged Figure 5 in cyan (about 4-nm thick CdS shell)). All films were acquired in the same conditions, and the statistics for each sample were done on at least 120 QDs using automated homemade software. Images were acquired continuously for 70 s at 33 Hz with a CCD camera.

As previously reported,[4,5] the main interest of CdSe/CdS core/shell structures with thick CdS shells is the strongly reduced blinking behavior they exhibit. To evaluate the effectivess of blinking reduction, 70 s movies (at 33 Hz frame rate) of well-dispersed nanocrystals on a cover-slit under an epi-fluorescence microscope (oil objective ×100) are recorded. Plotting the fraction of nonblinking quantum dots over time (Figure 8) allows an accurate comparison of the different samples described above. Compared to CdSe/ZnS nanocrystals (for which On times are no longer than 3 s), the three CdSe/CdS QDs samples are very stable and contain about 30% of dots which do not blink during 70 s. Again, we can conclude that the presence of stacking faults in the nanocrystal is not followed by creation of traps and does not affect the optical properties of a polytypic QD compared to a pure zinc-blende or wurtzite one.

Conclusion

We have described here two ways to obtain perfect wurtzite or zinc-blende CdSe/CdS nanocrystals with thick CdS shells. Advantages of working with the ZB setup are (i) the absence of primary amines in the growth solution suppresses the possibility of nucleation of CdS and (ii) this dropwise protocol is more comfortable to use and quicker for production of thick shells than multi-injections methods. Furthermore, we have shown in this study that surface ligands exchange on CdSe nanocrystals can induce a partial crystalline transition from zinc-blende to wurtzite structure. These structural modifications can be characterized using a spectroscopic argument (energy difference between the first and second excitons) and are supported by the observation of polytypism in CdSe/CdS core/shell nanocrystals when the shell synthesis protocol uses primary amines. It then becomes essential to know the initial core crystalline structure and the influence of shell ligands to improve the control of complex core/shell nanocrystals synthesis. These results, focused on CdSe core and primary amines as ligand, could be extended to other types of materials and surface ligands and could help to rationalize one step further the II−VI semiconductors nanocrystals synthesis.

Acknowledgment. We thank Mohamed Hanafi for precursors preparation and technical assistance, Patrick Bassoul for electron

(27) Fedorov, V. A.; Ganshin, V. A.; Korkishko, Y. N. *Phys. Status Solidi A* **1991**, *126*, K5–K7.
(28) Bandaranayake, R. J.; Wen, G. W.; Lin, J. Y.; Jiang, H. X.; Sorensen, C. M. *Appl. Phys. Lett.* **1995**, *67*, 831–833.
(29) Al-Salim, N.; Young, A. G.; Tilley, R. D.; McQuillan, A. J.; Xia, J. *Chem. Mater.* **2007**, *19*, 5185–5193.
(30) Talapin, D. V.; Nelson, J. H.; Shevchenko, E. V.; Aloni, S.; Sadtler, B.; Alivisatos, A. P. *Nano Lett.* **2007**, *7*, 2951–2959.
(31) Fiore, A.; Mastria, R.; Lupo, M. G.; Lanzani, G.; Giannini, C.; Carlino, E.; Morello, G.; De Giorgi, M.; Li, Y.; Cingolani, R.; Manna, L. *J. Am. Chem. Soc.* **2009**, *131*, 2274–2282.

microscope management, the Human Frontier Science Program, and l'Agence Nationale de la Recherche and La Région Ile-de-France for funding. B.D. thanks Eric Doris and Stephanie Foillard for help with XPS measurements and analysis.

Supporting Information Available: Synthesis protocol, and characterizations of large ZB CdSe nanocrystals; FT-IR spectra of ZB CdSe nanocrystals before and after ligand exchange with oleylamine; fitting procedure for the determination of $E_2 - E_1$; crystal structure determination using HRTEM pictures; TEM pictures of ZB CdSe/CdS spherical nanocrystals; XPS analysis of CdSe/CdS. This material is available free of charge via the Internet at http://pubs.acs.org.

JA9034973